



AIAA 2002-4173
COMBUSTION MECHANISMS OF BIMODAL
AND ULTRA-FINE ALUMINUM IN AP SOLID
PROPELLANT

A. Dokhan, E. W. Price, J. M. Seitzman,
and R. K. Sigman
School of Aerospace Engineering
Georgia Institute of Technology
Atlanta, GA

38th AIAA/ASME/SAE/ASEE
Joint Propulsion Conference and Exhibit
July 7-10, 2002 / Indianapolis, IN

Combustion Mechanisms of Bimodal and Ultra-Fine Aluminum in Ammonium Perchlorate Solid Propellant

A. Dokhan^{*}, E.W. Price[†], J. M. Seitzman[‡] and R.K. Sigman[§]

Georgia Institute of Technology
School of Aerospace Engineering
Atlanta, Georgia 30332-0150

ABSTRACT

An experimental investigation was carried out to evaluate the combustion behavior of aluminized, ammonium perchlorate composite propellants, with various Al particle sizes, including bimodal aluminum size distributions using ultra-fine aluminum (UFAl, $\sim 0.1\mu\text{m}$) as the fine component. It was found that the burning rate could be increased several fold with UFAl, with major increases produced by an aluminum blend *with only 20% UFAl* under some conditions. Presence of UFAl had a major effect on the appearance of the flame, and on the amount and size distribution of the Al_2O_3 product particles. Explanations of the burning rate effect of fine Al are proposed that involve rapid Al combustion, and include Al ignition and oxidizer availability as important variables. Some possible causes of the effects on the product oxide size are also discussed.

INTRODUCTION

Powdered aluminum is used in solid rocket propellants because of the high-energy release in its oxidation to Al_2O_3 , and its high density compared to other ingredients. While the condensed state of the product is generally disadvantageous, the droplets are effective damping agents for oscillatory combustor instabilities. The combustion of conventional sized Aluminum ($15\mu\text{m}$ - $95\mu\text{m}$) does not ordinarily contribute much to the propellant burning rate because its burning occurs relatively far from the propellant surface. Introduction of aluminum (Al) to an already fuel rich system tends to reduce burning rates. In this report, one of the primary goals is evaluation of a potential method to enhance heating of the burning surface (and thus increase the burning rate) by producing Al burning closer to surface. In pursuing this goal, it should be recognized that the behavior of Al in the propellant combustion zone has been studied extensively because it is important to combustion efficiency, combustion stability, slag formation, two phase flow losses, component erosion, and potentially to burning rate. In order to understand the results of the present study, it is necessary to be aware of several properties and behavior of Al and its oxides as described in Refs. 1-5 and summarized below.

Unlike other propellant ingredients, Al does not vaporize at the temperatures present in the propellant

^{*} Ph.D Candidate. Student Member.

Email: allandokhan@hotmail.com

[†] Regent Professor Emeritus. Fellow AIAA Member.

[‡] Associate Professor. Senior AIAA Member.

[§] Senior Research Engineer

surface ($\sim 600^\circ\text{C}$). It is seen to adhere to the burning surface temporarily, giving an opportunity for particle concentration and adhesion. This creates an opportunity for formation of aggregates of various sizes (2 to 10^6 particles) that are converted to burning "agglomerate" droplets as they move into high temperature regions of the combustion zone.

Aluminum is extraordinarily reactive, but this oxidation is impeded at low and intermediate temperatures by formation of an impervious oxide "skin" on the particles that does not melt until a temperature of 2047°C is reached. Some reaction occurs at the melting point of the Al (660°C), due to its expansion ($\sim 6\%$) during phase change. This causes leaking and surface oxidation of molten Al at the cracks in the oxide skin (Fig. 4 of Ref. 2). This creates an opportunity for concentrations of particles (now droplets confined in their oxide skins) to sinter together into "aggregates." When the aggregates reach 2047°C , the surface tension of the Al converts the aggregate to one or more droplets (agglomerates) and the surface tension of the insoluble oxide causes it to retract to one or more lobes on the aluminum droplet surface. The extent of aggregation is affected by the degree of initial Al concentration within the packing pattern of the larger AP particles in the propellant, and by proximity of high temperature sites in the array of flamelets above the surface. These factors are controllable to some extent by selection of oxidizer and Al particle size distribution, and the sintering is affected appreciably by the initial thickness of the oxide skin.

The increasing exposure of Al during breakdown of the oxide skin leads to precipitous increases in Al oxidation and to self-heating and temperature increase of the droplet. At some point the vaporization rate of the Al becomes high enough to shift the site of oxidation to the gas phase, where the product oxide forms oxide “smoke” (Al_2O_3 droplets in the under $2\mu\text{m}$ range). Once inflammation starts at a site in the aggregate, complete transformation to a burning agglomerate (ignition?) is rapid (1-2 ms for large aggregates), and usually coincides with the moment of detachment from the surface (in AP propellants). Aggregates ignite earlier and form smaller agglomerates at higher pressures, presumably because the hot gas phase flamelets stand closer to the burning surfaces.

In recent years, nano-sized Al particles ($\sim 0.1\mu\text{m}$) have gained considerable attention because of potentially significant increases in propellant burning rates. However, the rocket community has generally rejected its use as a feasible working Al particle because of a higher content of unwanted Al_2O_3 oxide coating that ultimately reduces the maximum achievable specific impulse of the propellant. The goal of the present study was to demonstrate mechanistically the ability of tailoring propellant formulations towards specific applicational needs, and, provide guidelines for formulating propellants with high burning rates for rapid launch and with minimal losses to performance. The research involved the use of nano-sized and conventional sized Al at various mass distributions.

EXPERIMENTAL APPROACH

Combustion tests were run in a conventional nitrogen-flushed window bomb and in the Georgia Institute of Technology particle collection apparatus. Combustion in the window bomb was viewed by a high-speed digital camera, and the size distributions of the collected particles were determined in a specially designed apparatus that included microscopic examination.⁶

WINDOW BOMB TESTS

The test apparatus has been described in many reports.^{3,6} Tests were run at four pressures (6.9MPa, 5.52MPa, 3.45MPa and 1.38MPa). Test samples were 11mm tall, 7mm wide and 4mm thick and were burned from the top downward. They were lightly inhibited on the sides with silicone gel. A high-speed camera was needed to get enough frames in high burning rate tests to measure rate (1000fps). In addition, some trouble was encountered with the extreme brightness of the flame with formulations containing UFAl (it was necessary to use small lens

aperture, short exposure time and filtering). Some samples burned unevenly, and rates were measured at multiple surface sites.

PARTICLE COLLECTION TESTS

The test apparatus consisted of a 50.8mm ID steel cylinder, vertically mounted, with a coaxial 25.4mm ID quartz tube (584.2mm long) suspended at the upper end. The cylindrical propellant sample (25.4mm, 10mm thick) was mounted in the upper end of the quartz tube^{6,7}. The sample was ignited on the downward facing side and the combustion plume flowed out the open end at the bottom of the quartz tube. A pool of ethanol was maintained below the mouth of the tube. The exiting plume reversed its direction there, and flowed upward and vented into a surge tank. Most of the submicron “smoke” oxide exited with the gas and some smoke and the oxide particles greater than $2\mu\text{m}$ impinged on the ethanol and remained in the collected sample. Particles remaining in the quartz tube were washed out with ethanol and added to the collected sample. The fine smoke oxide remaining in the sample was separated from the larger particles remaining from aluminum droplet burnout (“residual oxide particles”) using a sedimentation separation procedure. This method is feasible with the larger aluminum particle sizes used here because of the large differences between the particle sizes of smoke oxide and burnout residuals. The burnout residuals for particles of the ultra fine Al (UFAl) used here would be so small that the method of separation from smoke oxide used here would not work (unless massive aluminum agglomeration occurred).

Size distribution of the residual oxide particles was accomplished as follows:

- a) weigh the total residual oxide collected (after sedimentation);
- b) separate into three size subsamples ($106\mu\text{m} < D < 212\mu\text{m}$, $45\mu\text{m} < D < 106\mu\text{m}$, and $10\mu\text{m} < D < 45\mu\text{m}$) by screening;
- c) weigh the three subsamples;
- d) disperse each subsample onto a microscopic slide and determine the diameter of each residual oxide product using “Image Pro Plus” software;
- e) Using an ‘in house’ written software, calculate a number-count (the number of particles that are counted range from 1000-1500 particles to 20000-40000 particles for sieve ranges $106\mu\text{m} < D < 212\mu\text{m}$ and $10\mu\text{m} < D < 45\mu\text{m}$ respectively) and a mass

distribution, and adjust to the previously measured subsample mass;

- f) convert to normalized mass-weighted size distribution by mass measurements by particle size and dividing by the total oxide mass possible assuming all the aluminum in the propellant sample is converted to Al_2O_3 – thus, the area under the distribution function curve is the mass fraction of oxide ending up in the residual oxide particle form.

PROPELLANTS

All propellants were 11% PBAN binder, 18% aluminum (Al) and 71% ammonium perchlorate (AP) (high purity, no anticaking agent). The AP was of bimodal particle size distribution with 400 μ m (coarse) and either 82.5 or 10 μ m (fine). In most samples, the Al was of bimodal size distribution with 30 μ m and 0.1 μ m (UFAl, also referred to as Alex) particles. One series of four mixes used monomodal Al, sizes 30 μ m, 15 μ m, 3 μ m and 0.1 μ m. The principal formulation variables were mass ratio of AP coarse to fine (AP c/f) and Al coarse to fine (Al c/f), and, AP fine particle size (82.5 μ m or 10 μ m). A total of 26 formulations were mixed. All gave satisfactory samples except the one with Al c/f = 0/100 and AP c/f = 80/20(10 μ m fine AP). The propellant was prepared by a combination of hand-mixing, machine mixing and vacuum pressing, detailed in Reference 6 and 8.

The choice of formulation variables was important because it is a means to “tweak” the microstructure of the combustion zone on a scale that is too small for practical real-time experimental measurements. 400 μ m coarse AP was chosen because it provided room in the propellant microstructure for a range of fines AP sizes. Bimodal size distribution was used in order to make the characterization of the microstructure relatively easy. 82.5 μ m fine AP was chosen because earlier studies^{3,9,10} had indicated that such particles burn with their own diffusion flamelets, while 10 μ m particles do not. Bimodal Al size distribution offered an opportunity to tailor burning rate, and oxide product particle sizes, and to use UFAl to obtain high burning rate.

EXPERIMENTAL RESULTS

Tests included approximately 144 window bomb tests on 26 formulations, at four pressures. Results presented here include several oxide flame images,

and burning rate for each test. Thirteen particle collection tests were run, mostly at 200psi. Particle size distributions were determined, and high magnification imaging was performed with optical and scanning electron microscopes.



(a)



(b)



(c)

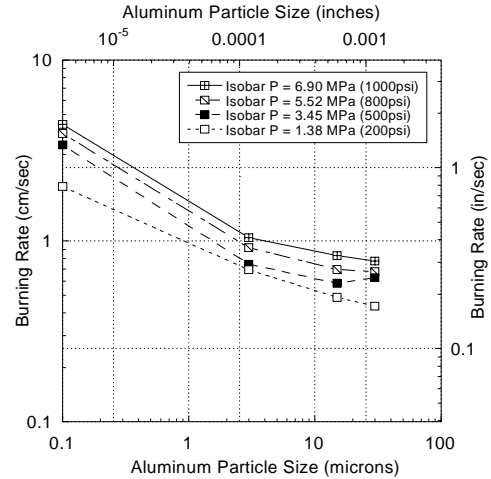


(d)

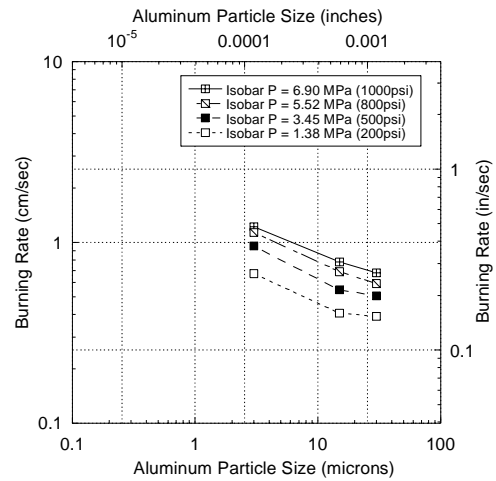
Figure 1. Images (3mm high) of the combustion zone for four different aluminum particle sizes (a) 30µm, (b) 15µm, (c) 3µm and (d) UFAI (~0.1µm); AP c/f ratio=80(400µm)/20(82.5µm) at 1.38MPa (200psi).

EFFECT OF AL PARTICLE SIZE

Propellant mixes were prepared with monomodal Al, using AP c/f ratio of 80/20. For the samples with 30µm and with 15µm Al, combustion photography showed Al droplets leaving the surface with some of agglomerate size (see Figure 1a, b). With 3µm Al, the region above the burning surface was almost uniformly luminous (see Figure 1c). With UFAI (~ 0.1µm) (see Figure 1d), the region above the surface was intensely luminous, starting very close to the surface and extending out for 1000µm. The burning rates for formulations with 82.5µm fine AP are shown as a function of Al particle size in Figure 2a for four pressures. The burning rate with 30µm and 15µm Al are about the same, while the rates with 3µm Al were somewhat higher and the rates with UFAI were dramatically higher (on average 440% higher compared to propellants with 30µm Al). The results suggest that the burning rate enhancement is due to the intense radiation field and elevated temperature near to the surface (this does not preclude the possibility that some Al oxidation and heat release at the surface contributed to the enhanced burning rate). Tests similar to the above were run on samples with 10µm fine AP (except the sample with UFAI, which was poorly consolidated). The photo images were similar to those with 82.5µm fine AP, and the burning rates were also similar (Figure 2b).

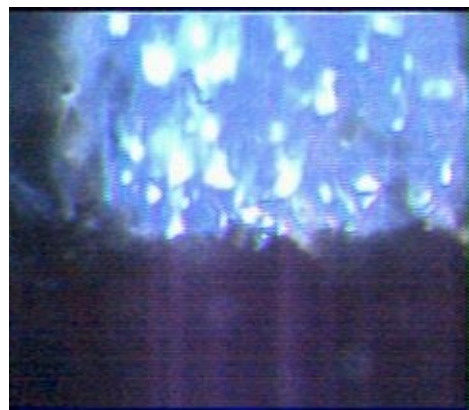


(a)



(b)

Figure 2. Burning rate as function of Al particle size for four pressures: a) fAP=82.5µm, b) fAP=10µm.



(a)



Figure 3. Images of the combustion zone for four different ratios of Al c/f mass ratio (a) 100/0, (b) 80/20, (c) 50/50 and (d) 0/100; (cAl=30μm, fAl=UFAI, fAP=10μm).

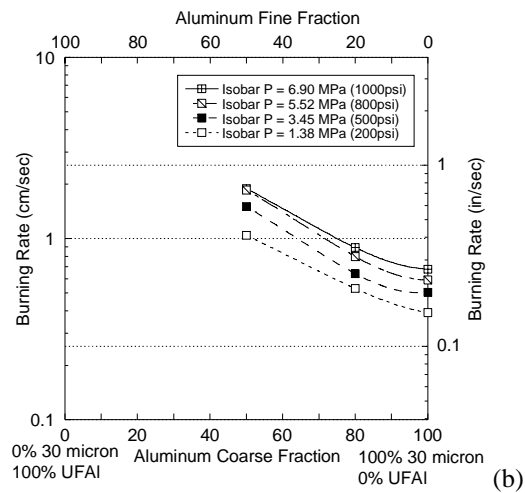
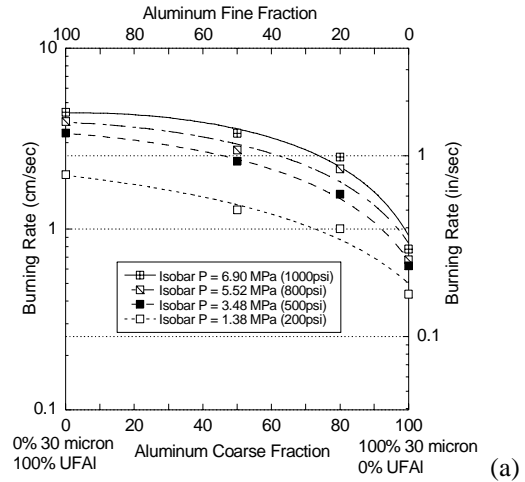


Figure 4. Burning rate as a function of ratio between coarse and fine Al: (a) fAP=82.5μm, (b) fAP=10μm; (for four different pressures).

BIMODAL AL: EFFECT OF RATIO OF COARSE TO FINE AL

Formulations with bimodal Al particle size distributions used 30μm Al and UFAI in different blends. The combustion imaging showed an intense radiation region just above the burning surfaces, increasingly dense as the amount of UFAI was increased (Figure 3). Figure 4(a) shows the burning rates as a function of coarse-to-fine Al ratio (Al c/f) for four pressures using AP c/f = 80/20 with 82.5μm fine AP (fAP). Figure 4(b) show the rates using 10μm fAP. With 82.5μm fAP, replacement of 20% of the 30μm Al with UFAI (Al c/f = 80/20) resulted in a ~150% increase in burning rate. Further increases in

UFAl produced progressively smaller additional increases in burning rate.

For the tests on formulations similar to the above, but with 10µm fAP, images (Figure 3b) showed an intensely bright Al flame for even 20% replacement of 30µm Al by UFAl. For higher amounts of UFAl, the image quality was poor due to smoke recirculation and image overexposure. For 0% UFAl, the burning rates in Figure 4(a) and (b) are about the same for either size fAP, but replacement of 20% of the 30µm Al with UFAl in the 10µm fAP formulation produced only a 30% increase in rate. The 10µm fAP propellant rates appeared to be “overtaking” the 82.5µm fAP at Al c/f=50/50.

EFFECT OF AP COARSE TO FINE RATIO

Tests were run for 82.5µm fAP samples with 80/20, 60/40 and 50/50 AP c/f, for three different Al c/f mass ratio (100/0, 80/20 and 50/50). The burning rates are shown in Figure 5a-c. As above, the rates increase with increasing fine Al loading (decrease in Al c/f). A notable feature of the burning rate trends in Figure 5 is the low sensitivity of burning rate to AP c/f for these propellant containing 82.5µm fAP. Similar tests were run for 10µm fAP samples. The burning rates are shown in Figure 6a-c. Unlike the corresponding results with 82.5µm fAP, the rate with 10µm fAP increases considerably with decreasing AP c/f (increasing fAP), as well as with increasing fAl. The fAl effect could have been anticipated from the 82.5µm fAP results, but the sensitivity to increasing fAP in the case of 10µm fAP seems to be an important clue to relevant combustion mechanisms.

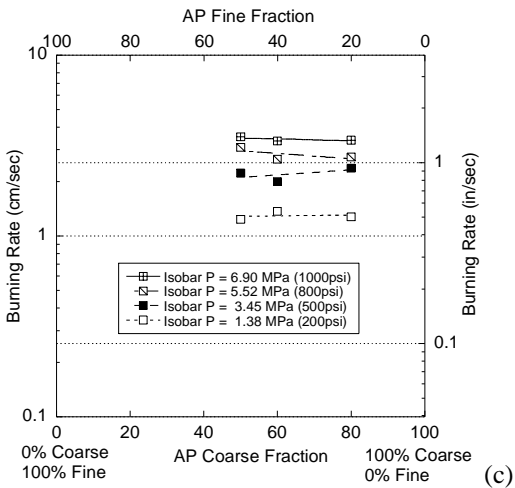
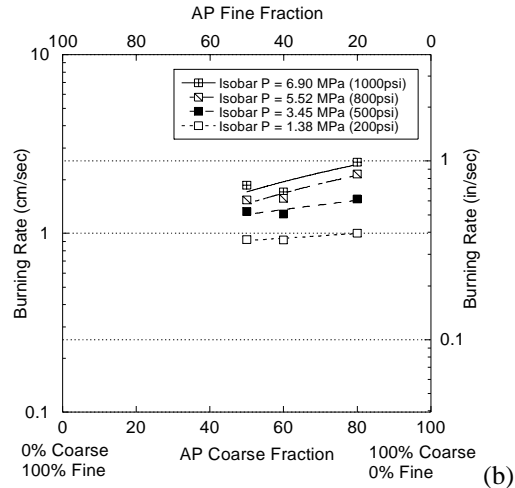
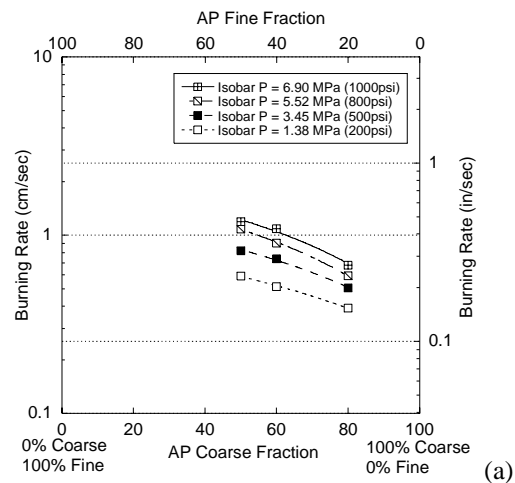
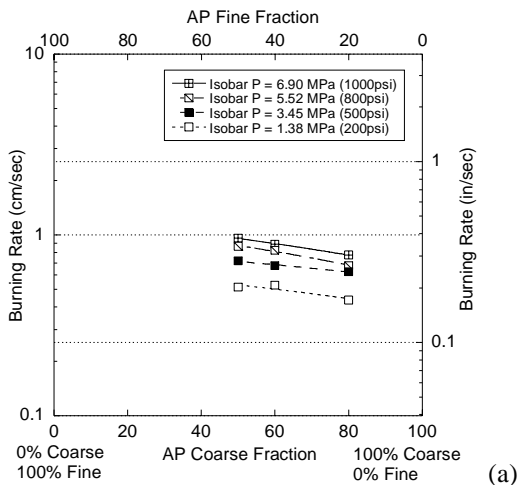


Figure 5. Burning rate as function of ratio between coarse and fine AP: (a) Al c/f ratio 100/0, (b) Al c/f ratio 80/20 and (c) Al c/f ratio 50/50; (cAP=400µm, fAP=82.5µm. cAl=30µm, fAl=UFAl).



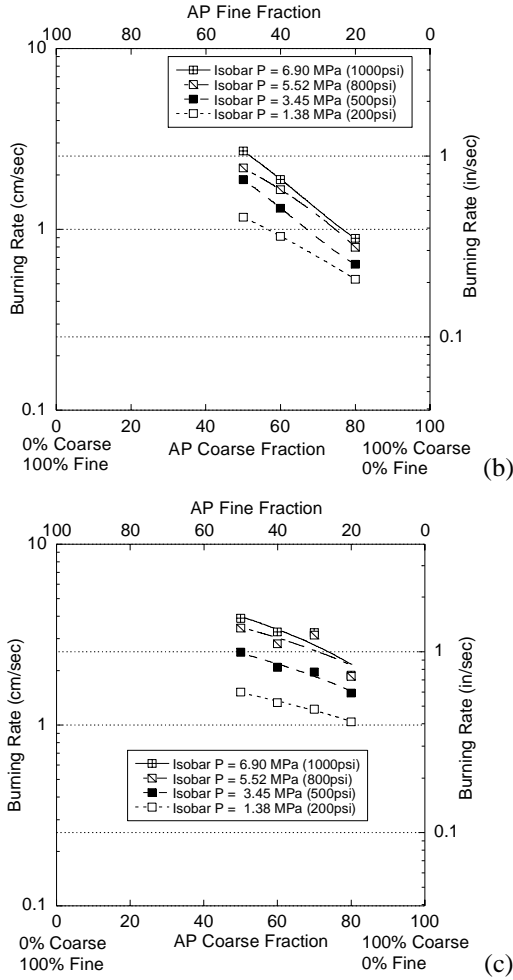


Figure 6. Burning rate as function of ratio between coarse and fine AP: (a) Al c/f ratio = 100/0, (b) Al c/f ratio 80/20 and (c) Al c/f ratio 50/50, for four different pressures (cAP=400µm, fAP=10µm. cAl=30µm, fAl=UFAl).

COLLECTED COMBUSTION RESIDUE

As noted earlier, the particle collection tests are designed to collect the larger Al₂O₃ combustion products, and a separation process is used to remove the “smoke” oxide. In the separation process, it was noted that the population of larger particles included some aggregate of small particles. This was unique to the propellants that contained UFAl, and the amount of aggregates increased with the amount of UFAl. Based on a microscopic examination, it was concluded that the aggregates were made up of fine particles, and they were removed before the determination of size distribution of the “residual” oxide droplets (see next section).

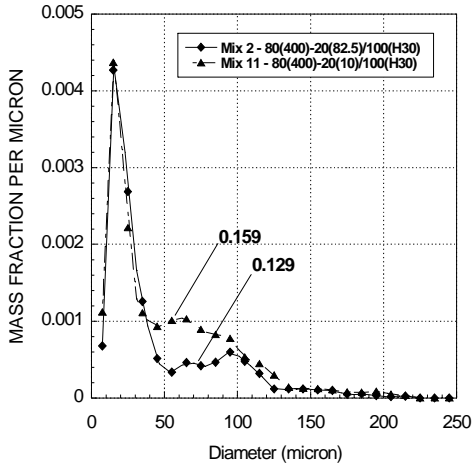
Figure 7 shows the mass size distributions for seven sets of formulations. The first (Figure 7a)

shows size distributions for two formulations that differ only in particle size of the fAP (AP c/f =80/20, Al = 30µm). The initial peak (~20µm) corresponds to the expected size of residual oxide from burn-out of single 30µm Al particles and the larger particles correspond to burn-out of agglomerates. The numbers identified with the curves correspond to the mass fraction of total oxide that consists of these residual particles (“total oxide” refers to the mass of oxide that would result from oxidation of all the aluminum in the propellant sample). In Figure 7a, 15.9% and 12.9% of the oxide were in the form of residual particles, the lesser amount being for the formulation with 10µm fAP.

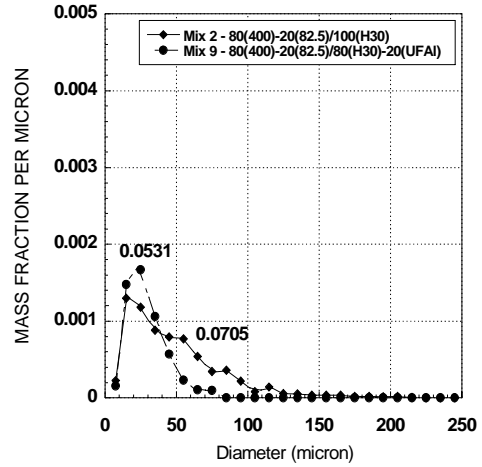
Figure 7b (fAP=82.5µm) and Figure 7c (fAP=10µm) shows the size distribution for formulations with various ratios of 30µm and UFAl (AP c/f =80/20, P=1.38MPa [200psi]). Compared to the samples with unimodal 30µm Al, two things are notable. One is the reduction of the peak at 20µm when UFAl is present in the formulation, and the other is the decrease in residual oxide (“missing oxide”). Figure 7d and Figure 7e shows the residual oxide size distributions for two of the bimodal formulations shown in Figure 7b and Figure 7c respectively, but at 500psi. The most notable difference is the lower mass of residuals at higher pressure. Figure 7f (fAP=82.5µm) and Figure 7g (fAP=10µm) shows the residual oxide distribution for propellants with Al c/f ratio of 50/50 with various AP c/f mass ratios (80/20 and 60/40) at 1.38MPa [200psi]. The results show no significant differences to the diameter to which the first peak occurs and there is a significant reduction in the amount of residual mass collected.

OXIDE AGGREGATES

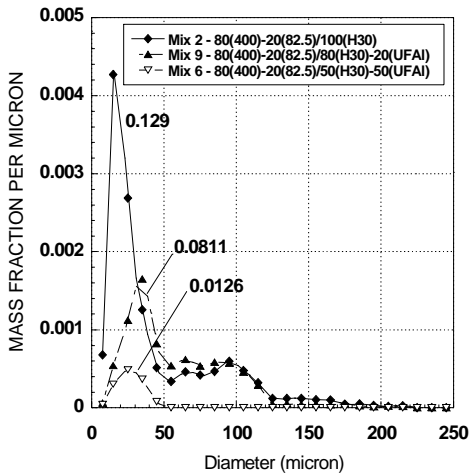
As noted above, large aggregates of fine oxide particles appeared in the residual oxide samples when UFAl was included in the propellant. The aggregates were collected and weighed for each test as noted above. Their mass increased when the UFAl content was increased; the collected aggregate mass was comparable to the total residual mass at intermediate UFAl content, and was the only mass remaining when all the Al was UFAl (Figure 8).



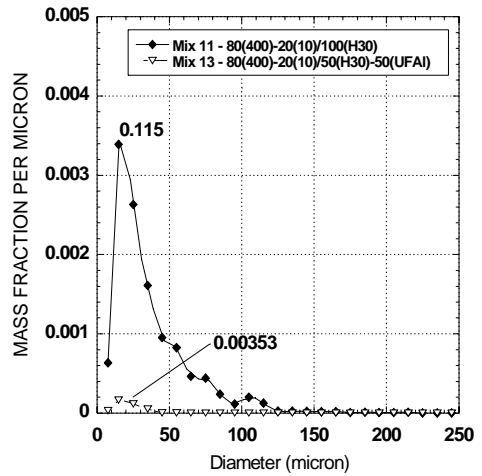
(a)



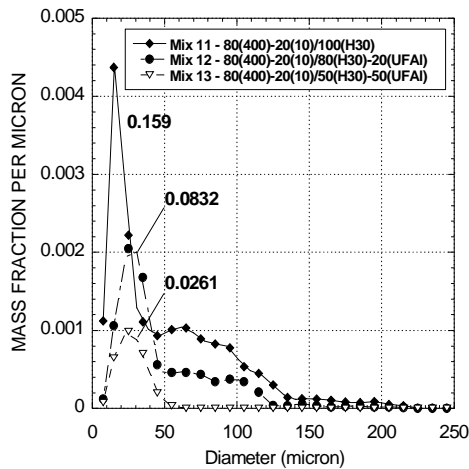
(d)



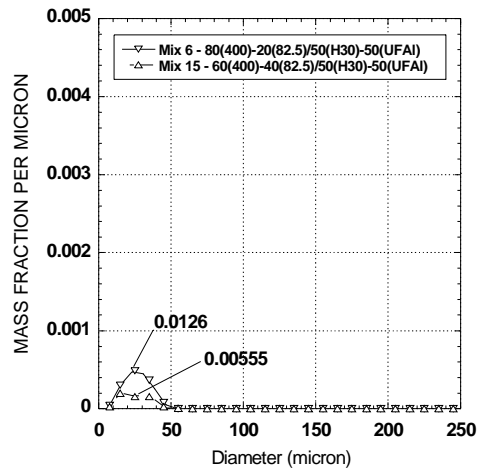
(b)



(e)



(c)



(f)

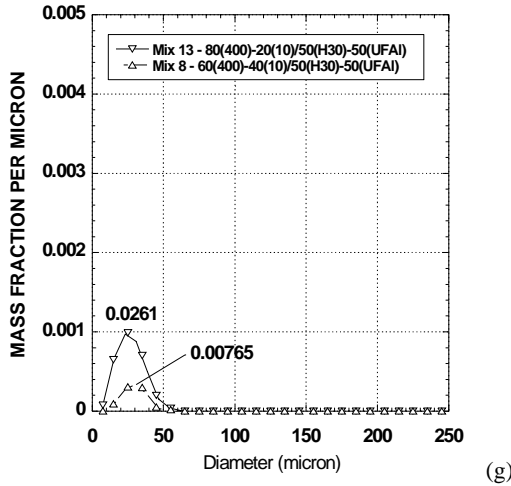


Figure 7. Mass-size distribution of residual oxide particles for propellants with AP c/f ratio=80/20:a) varying fAP with 30 μ m Al (at 200psi); varying Al c/f (30 μ m Al and UFAl) with: b) fAP=82.5 μ m (200psi); c) fAP=10 μ m (200psi); (d) same as (b) at 500psi; (e) same as (c) at 500psi; and for propellants with Al c/f ratio=50/50, varying the AP c/f ratio with: (f) fAP=82.5 μ m and (g) fAP=10 μ m.

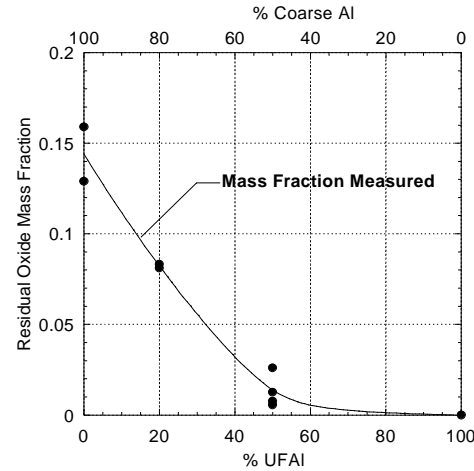


Figure 8. Mass of oxide aggregates as function of fraction of UFAl in tests on propellants of various Al c/f ratio and AP c/f ratio.

In an effort to determine how the aggregates were formed, the UFAl was examined with a scanning electron microscope (Figure 9a), which showed a substantial content of “clumps” the fate of these clumps in the propellant mixing process and/or combustion zone is problematic. The aggregates in the collected oxide were also examined (Figure 9b), and found to consist of particles in sizes up to ~8 μ m. The larger ones appeared to be oxide spheres. The aggregates survive various bulk modes of agitation, but could be broken up by probing with a pointed tool.

INTERPRETATION OF RESULTS

THE COMBUSTION ENVIRONMENT FOR ALUMINUM

In the Introduction, it was pointed out that the reaction rate of Al particles is limited by the presence of an oxide “skin” that does not break down until the particle (now a droplet) nears the melting point of the oxide (2047 $^{\circ}$ C). Those temperatures occur in the gas phase flame above the propellant surface, a flame consisting of an array of flamelets formed in the microscopic mixing flows that emerge from the oxidizer/binder boundaries on the surface. From the standpoint of Al ignition, the sites in the flamelet array that most affect propellant burning rate are those that are: a) hot, b) near the surface, and c) have both Al and oxidizer present. This is illustrated in the flamelet sketch in Figure 10.

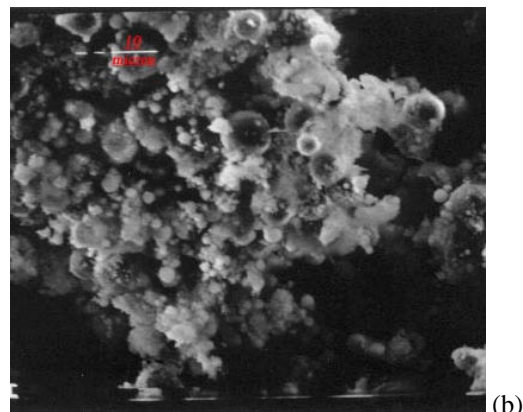
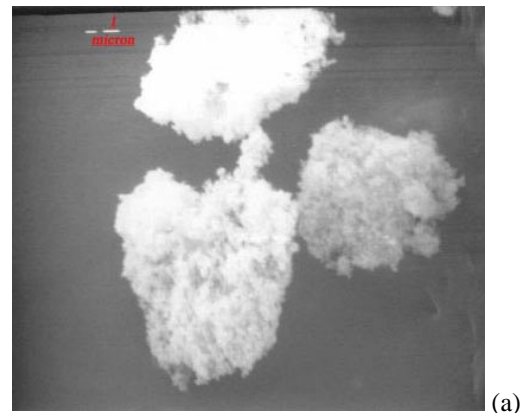


Figure 9. Scanning electron microscope image of: a) unburned UFAl “clumps” (second bar at upper left represents 1 μ m); b) product oxide aggregate from collection test on propellant containing only UFAl (third bar at upper left represents 10 μ m).

Figure 10 shows an AP particle and an adjoining region of binder, Al, and fine AP, referred to as a “matrix.” In this sketch, it is assumed that the Al and AP particles are so small that the matrix out-flow is premixed. As the AP and matrix vapors move outward, a “mixing fan” develops between them, designated here by constant composition lines,** including a line for stoichiometric mixture ratio. Oxidizer/binder reaction rates very close to the surface are low because temperature is “low” in the chemical kinetic sense. However, the mixing rate is very high in the leading edge of the mixing fan due to high lateral concentration gradient, leading to development of a local concentration of mixture that is large enough to support a flame (designated in the sketch as the “leading edge flame,” or “LEF”). The LEF is located 50 μm or so from the surface, and a classical diffusion flame trails out along the stoichiometric line in the mixing fan. The LEF is important to the Al combustion problem because it is the nearest site to the surface that produces temperatures high enough to melt the oxide skin on the Al, permitting Al combustion. Some other important features of the LEF are (relative to the sketch):

- oxidizer-rich extension to the left (no Al there) with progressively lower temperature to the left;
- fuel rich extension to the right that either: i) trails off into a matrix flame if the oxidizer content of the matrix is high enough to support a flame, ii) terminates where the mixture is too fuel rich for a flame, or iii) merges with a LEF from an adjoining coarse AP particle;
- LEF extends around the coarse AP particle, potentially transitioning from state i) to ii) to iii) according to: proximity of neighboring coarse AP particles, fine AP/binder ratio of the matrix, and prevailing pressure;
- if the fine AP particles are large enough or the pressure high enough, LEFs may establish in their mixing fans as well (based on previous work, it is likely that the 82.5 μm fine AP establish LEFs under the current conditions, but not the 10 μm fine AP).

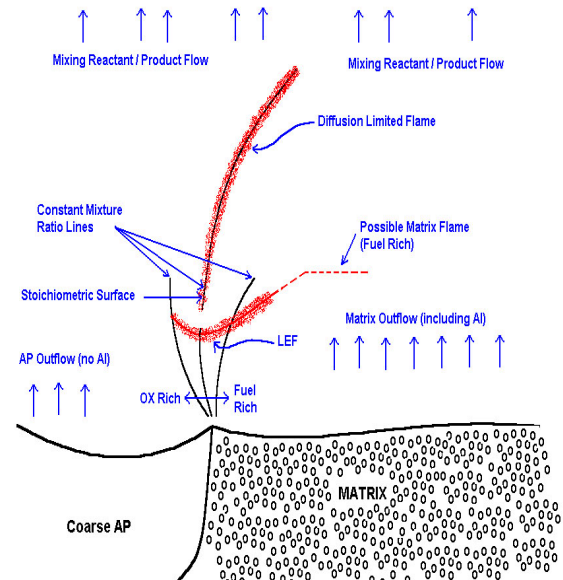


Figure 10. Schematic of expected microstructure of the combustion zone.

From the foregoing, it is evident that the flamelet “canopy” above the aluminum-containing mixture is highly convoluted and of nonuniform temperature and composition with the details strongly dependent on the oxidizer particle array on the surface. Al particles that leave the surface are convected outward toward the flame canopy. Their thermal environment depends on their approach path and arrival point at the flame canopy. Large Al particles experience both velocity and thermal lag as they move out from the surface and through the flame. Once ignited, they take a long time to burn. Fine Al particles maintain near-equilibrium (velocity and temperature) with the gas flow, ignite quickly as they pass through the flame surface, and burn close behind the flame. Keeping in mind that one 30 μm Al particle is the mass equivalent of 10^7 UFAl particles of 0.15 μm diameter, it is reasonable to postulate an extremely large Al combustion heat release close to the flame canopy when UFAl is used. However, the amount of near-surface heat release would be dependent on amount of UFAl, availability of oxidizing species, and proportion of the flame canopy that is near-surface and hot enough to ignite the Al.

EFFECT OF ALUMINUM PARTICLE SIZE

The tests involving monomodal Al particle size distribution showed a drastic difference in the Al “combustion field” with smaller particle size. The huge increase in the number of particles results in a very dense, luminous field close to the burning

**Refer to references 9, 11, 12 for detailed arguments on flame configuration.

surface, which produces a moderate increase in burning rate with $3\mu\text{m}$ Al, and a major increase in burning rate with UFAl. The arguments presented above indicate that the particles ignite at a distance from the surface determined by the AP/binder flame standoff distance, which is too small to resolve in the imaging. The UFAl particles have low thermal lag relative to the gas, so that the UFAl flame is close to the AP/binder flame and heats the propellant surface directly by radiation and also heats the AP/binder flame by conduction. In the formulations with 80/20 AP c/f, the surface area is dominated by the coarse AP particles. With the $82.5\mu\text{m}$ fAP, those particles are located in the largest voids in the coarse AP packing array, with the Al/binder mixture filling the smaller spaces. This array provides plentiful LEFs for igniting Al, but the burning rate of the Al cloud may be limited by the time (distance) for lateral diffusion of oxidizing species from the columns of out-flow from the oxidizer particles. When the $10\mu\text{m}$ fAP is used, the lateral diffusion time is lessened, but there is a shortage of LEF sites for igniting the Al. In this respect, it may be significant that ignition time is more important with coarse Al (which does not deplete the oxidizer so fast), while short diffusion time may be more important with fine Al (which depletes oxidizer rapidly). This may explain the moderate differences in burning rate of formulations with $82.5\mu\text{m}$ and $10\mu\text{m}$ fAP. However this interpretation may be only part of the story, because the rather modest effects of fAP particle size neglect the effect that fAP particle size has even in nonaluminized formulations, and the modest effects may be determined in part by the modest heat release on the surface in processes that lead to Al agglomeration. If one were to argue that the rate increase resulting from decrease in Al size was due to enhanced Al reaction on the propellant surface, then one would expect a much larger effect of Al particle size with $10\mu\text{m}$ fAP because of the greater availability of oxidizing species at the surface. The results show the effect was not large, thus suggesting Al reaction on the burning surface is too limited to explain the Al particle size effect.

EFFECT OF ALUMINUM COARSE TO FINE MASS RATIO

The trend of burning rate with replacement of $30\mu\text{m}$ Al with UFAl is consistent with the arguments regarding ignition sites and oxidizer diffusion. With AP c/f = 80/20, the formulations with $82.5\mu\text{m}$ fAP showed a large rate increase with 20% replacement and lessening increase for further UFAl increase.

This formulation would be expected to have plentiful Al ignition sites, but slow oxidizer diffusion due to the “large” size of the fine AP particles. Thus continuing increases in UFAl is less effective because of limited availability of oxidizing species near the surface in the UFAl outflows. For the formulations with $10\mu\text{m}$ fAP, diffusion times are not a problem, but ignition sites (LEFs) are less plentiful, leading to lower rates than with $82.5\mu\text{m}$ fAP.

EFFECT OF AP COARSE-TO-FINE RATIO

When higher proportions of fAP are used in the formulations, the burning rate still increases with increases of UFAl, but the rate increase is strongly dependent on amount and size of the fine AP (Figures 5 and 6). With $82.5\mu\text{m}$ fAP, the rate for each Al c/f was relatively insensitive to increase in fAP content, supporting the interpretation that the supply of LEFs is plentiful (i.e., high density of near-surface LEFs) but diffusion distances for oxidizing species into the UFAl out-flow limits near-surface UFAl combustion rate with $82.5\mu\text{m}$ fAP.

With $10\mu\text{m}$ fAP, diffusion distance is not the limiting factor on near-surface UFAl burning, low proximity of LEF ignition sites is (because LEF sites are present only on the $400\mu\text{m}$ AP particles). However, the burning rate increases with increasing fAP (decreasing cAP). This apparent contradiction between the rate trends with AP c/f ratio with $10\mu\text{m}$ fAP can be explained by reference to a more complete consideration of the flame canopy as described in the first subsection of this “Interpretation” section. When fAP is used in the matrix, the stoichiometric surface and the LEF shift towards the matrix, and the fuel-rich side extends further into the matrix flow as AP content of the matrix is increased. Based on results of sandwich burning tests, it seems likely that LEFs from adjoining $400\mu\text{m}$ particles are increasingly interactive as the fAP content in the matrix is increased. In addition, the temperature of the unsupported matrix flame may be high enough to ignite the UFAl when AP c/f reaches 50/50. Thus it is reasonable to propose that the flame canopy becomes a better near-surface heat source for UFAl ignition as matrix AP content is increased, even though the number of LEFs is decreasing. This is consistent with the slopes of the curves shown in Figure 6.

COLLECTED COMBUSTION RESIDUE

The conventional view is that Al droplets end their burning with a residual oxide droplet that is large compared to the smoke droplets that form in the

flame envelop around the droplet. The resident oxide on the burning droplet is attributed to a) the oxide “skin” originally on the ingredient Al particle (or particles if the burning droplet is an agglomerate), b) additional surface oxide formed while on the burning surface, c) formation of oxide on the surface during burning and d) diffusion of smoke oxide to the surface. The relative importance of these mechanisms is not established, and presumably may depend on (or be manipulated by) the propellant formulation and Al particle characteristics, and on combustion pressure. Figure 7a shows examples where 13 to 16% of the Al ended up in residual oxide form (fairly conventional propellants). The size distributions suggest that in this about half of the aluminum burned as single particles and half burned as agglomerates. However, the formulation with 10 μ m fAP showed more agglomeration (probably because of fewer LEF ignition sites).

In the simplest view, one might assume that replacing part of the 30 μ m Al with UFAl would produce additive effects; i.e., the 30 μ m Al would burn as before but there would be less of it. The UFAl would form a hot near-surface flame consisting of 10⁶ to 10⁷ more particles (then with 30 μ m Al) and the 30 μ m particles (plus agglomerates) would pass through that flame undeterred. The UFAl, being submicron, would burn down to submicron residuals and smoke. This simple view however is not supported by the results.

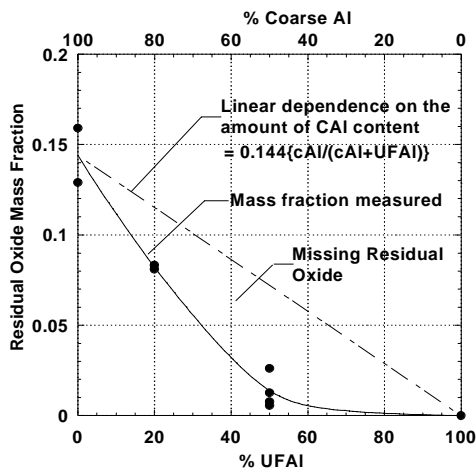


Figure 11: Mass fraction of residual oxide as function of fraction of Al that is UFAl.

Combustion photography shows relatively few of the 30 μ m droplets emerging from the UFAl flame layer, suggesting that something happened to them in the UFAl flame region (e.g. super-heating, accelerated burning, fragmentation). This is consistent with the decrease measured in residual oxide, which is more than would be expected based

on the decrease in 30 μ m Al in the formulation. This decrease in residual oxide is summarized in Figure 11, which shows the amount of residual oxide collected as a function of the fraction of Al in UFAl form. The top curve represents the residual oxide that would result if all 30 μ m Al produced the same mass fraction of oxide in residual form and matched to the 100% coarse Al results. The lower curve shows the measured mass fractions. The shaded area represents the difference or “missing” residual oxide. This nonlinear behavior of the residual oxide product is suggestive of anomalies in burning of 30 μ m Al particles induced by the UFAl flame.

These anomalies in burning of the coarse Al in the fine Al flame are a challenging fundamental problem. From a practical viewpoint, the behavior is advantageous relative to the slag, two-phase flow loss and combustion efficiency problems. Regarding the combustor stability problem, prediction of particulate damping is difficult because the amount and size of the residual oxide droplets become difficult to predict.

Regarding the oxide aggregate particles that were collected with the UFAl-containing propellants, their mass was not negligible (Figure 8). After considerable speculation about how they were formed, it was concluded that they must have been produced in the collection process. This conclusion was based on the reasoning that they would have formed into droplets if they had existed in the combustion zone. This raises the questions of: a) why do aggregates form when the propellants contain UFAl? and b) what is the origin of the particles in the aggregate? No answer is offered here to question a). Regarding b), if the aggregates are formed during collection (as argued above), the constituent particles are produced by the combustion and might be either the outcome of the anomalous coarse Al combustion, or a result of agglomeration of UFAl on the burning surface, or both. However, it should be noted that the samples examined with the SEM (Figure 9b) resulted from propellant with Al that was all UFAl, so the particles observed (8 μ m and smaller) apparently indicates “massive” UFAl agglomeration (10⁵ to 10⁶ particles).

CONCLUSIONS

This study was undertaken to determine the effect of using bimodal Al particle size distribution in propellants. Very fine Al (~0.1 μ m UFAl) was used as a means to increase burning rates, and Al of more conventional particle size was used with the expectation that it would provide product oxide droplets of appropriate size for damping combustion

instability. The family of formulation variables was chosen to facilitate understanding of the combustion process and use of that understanding to tailor formulations to meet specific applicational needs. The following are mechanistic insights that evolved from this study.

As Al particle size is decreased, the Al combustion takes place closer to the propellant burning surface, with a corresponding large increase in burning rate. With UFAl, an intense Al flame occurs near the surface, even when only 20% of Al is in this fine size. The study of effect of formulation variables indicates that the Al flame and its effect on burning rate are strongly dependent on the details of the oxidizer/binder vapor phase flame canopy over the burning surface. The Al outflow is ignited nearest to the surface at those sites in the flame canopy that are near the surface and very hot, with both Al and oxidizer species present. Such sites are determined by the ingredient proportions and particle sizes. Current qualitative theory of the flame structure and its relation to propellant micro-structure was used to explain the observed dependence of burning rate on propellant formulation variables.

Particle collection tests showed that around 15% of the product oxide was in ~10-100 μ m "residuals" from droplet burnout when conventional Al particles were used. Replacement of part of the conventional Al by 0.1 μ m Al posed the question of how this fine Al burned, whether it agglomerated, and how it interacted with the coarse Al. Presumably none of the oxide would be recovered in the residual oxide if the 0.1 μ m particles burned separately. The particle collection tests showed very strong particle interaction, not fully elucidated here. A "new" population of oxide particles in the less than 10 μ m range has emerged, possibly due to agglomeration of 0.1 μ m particles, or to fragmentation of the 30 μ m particles (droplets). The population of conventional oxide residuals is disproportionately reduced by partial replacement with 0.1 μ m Al. Appearance of this anomaly is accompanied by a marked decrease in burning droplets in the flow beyond the bright Al flame produced by the 0.1 μ m Al. This suggests some kind of disruption of burning of the 30 μ m Al as it passes through the 0.1 μ m particle flame. Taken collectively, the results provide good insight into enhancement of burning rate by use of fine Al size, and indicate that introduction of 0.1 μ m Al can dramatically change the amount and size distribution of the residual oxide droplets.

ACKNOWLEDGEMENTS

A. Dokhan gratefully acknowledges financial support from the Georgia Tech School of Aerospace Engineering. Thanks are also due to Argonide Corp., Valley Metallurgical Co., WECCO, Naval Air Weapons Center and Thiokol Corp. for supplying the UFAl, conventional aluminum, coarse AP, 10 μ m AP and binder respectively.

REFERENCES

- ¹Price, E.W., "Combustion of Metallized Propellants," *Progress in Astronautics and Aeronautics*, Vol. 90, 1984.
- ²Price, E.W., and Sigman, R.K., "Combustion of Aluminized Solid Propellants," *Progress in Astronautics and Aeronautics. Solid Propellant Combustion, and Motor Ballistics*. Vol. 185, pp. 663-687.
- ³Sambamurthi, J.K., Price, E.W., and Sigman, R.K., "Aluminum Agglomeration in Solid Propellant Combustion," *AIAA Journal*, Vol. 22, Aug. 1984, pp. 1132-1138.
- ⁴Beckstead, M.W., Newbold, B.R., and Waroquet, C., "A Summary of Aluminum Combustion," 37th JANNAF Combustion Meeting, Chemical Propulsion Information Agency, Laurel, MD, Nov. 2000.
- ⁵Babuk, V.A., Vassiliev, and Sviridov, V.V., "Formation of Condensed Combustion Products at the Burning Surface of Solid Rocket Propellant," AIAA, 2000.
- ⁶Dokhan, A., "The Effects of Aluminum Particle Size on Aluminized Propellant Combustion," Doctoral Thesis, Georgia Institute of Technology, May 2002.
- ⁷Dokhan, A., Price, E.W., Sigman, R.K., and Seitzman, J.M., "The Effects of Al Particle Size on the Burning Rate and Residual Oxide in Aluminized Propellants," AIAA2001-3581 at the 37th AIAA/ASME/SAE/ASEE Joint Propulsion Conference and Exhibit, July 2001.
- ⁸Sigman, R.K., Jeenu, R., and Price, E.W., "A Small Scale Solid Propellant Mixer and Vacuum Degasser," Proceedings of the 36th JANNAF Combustion Meeting, Chemical Propulsion Information Agency, Laurel, MD, CPIA Pub. 231, Nov. 1999.
- ⁹Price, E.W., Chakravarthy, S.R., Sambamurthi, J.K., Sigman, R.K., and Panyam R.R., "The Details of Combustion of Ammonium Perchlorate Propellants: Leading Edge Flame Detachment," *Combustion Science and Technology*. Vol. 138, pp. 63-83, 1998.
- ¹⁰Lee, S.T., Price, E.W., and Sigman, R.K., "Effect of Multidimensional Flamelets in Composite Propellant Combustion." *Journal of Propulsion and Power*, Vol. 10, No. 6, Nov.-Dec. 1994.

¹¹Price, E.W., Sambamurthi, J.K., Sigman, R.K. and Panyam, R.R., "Combustion of Ammonium Perchlorate-Polymer Sandwiches," *Combustion and Flame*, Vol. 63, pp. 381-413, 1986.

¹²Price, E.W., "Effect of Multidemsional Flamelets in Composite Propellant Combustion." *Journal of Propulsion and Power*, Vol. 11, No. 4, pp. 717-728, 1995.